

Available online at www.sciencedirect.com**SciVerse ScienceDirect**

Energy Procedia 21 (2012) 58 – 65

Energy

Procedia3rd Workshop on Metallization for Crystalline Silicon Solar cells

25 – 26 October 2011, Charleroi, Belgium

Large area copper plated silicon solar cell exceeding 19.5% efficiency

L. Tous^{a,b,*}, R. Russell^a, J. Das^a, R. Labie^a, M. Ngamo^c, J. Horzel^a, H. Philipsen^a,
J. Sniekers^b, K. Vandermisssen^a, L. van den Brekel^d, T. Janssens^a, M. Aleman^a,
D.H. van Dorp^a, J. Poortmans^{a,b}, R. Mertens^{a,b}

^a*Imec vzw, Kapeldreef 75, Leuven B-3001, Belgium*^b*Katholieke Universiteit Leuven (KUL), Oude Markt 13 Bus 5005, Leuven 3000, Belgium*^c*TOTAL, 2 Place Jean Millier – La defense, Paris La defense 92078, France*^d*Meco Equipment Engineers BV, Marconilaan 2, Drunen 5151 DR, The Netherlands*

Abstract

This work focuses on using copper (Cu) as the main conductor as an alternative to standard screen printed silver (Ag) front contacts for homogeneous emitter silicon solar cells.

Two different approaches to form Cu plated contacts based on laser ablation of the SiNx:H antireflection coating (ARC) and subsequent plating steps are presented. In the first approach, contacts are formed by Ni/Cu/Ag plating in an industrial in-line plating tool and subsequent rapid thermal annealing (RTA). In the second approach, the RTA step is performed after sputtering of a thin nickel layer and prior to the final Ni/Cu/Ag plating sequence. Using the latter approach, results are presented on large area 12.5x12.5 cm² *p*-type CZ-Si PERC-type solar cells featuring an advanced 120 Ω/sq homogeneous emitter and local Al contacts on the rear surface accompanied by a SiOx/SiNx rear side passivation stack. Solar cell efficiencies of up to η=19.6% and average pull tab adhesion results >2 N are reported.

© 2012 Published by Elsevier Ltd. Selection and/or peer review under responsibility of Guy Beaucarne

Open access under [CC BY-NC-ND license](https://creativecommons.org/licenses/by-nc-nd/4.0/).

Keywords: Metallization; copper; Ni-Si/Cu contacts; PERC-type solar cells; deep homogeneous emitters

* Corresponding author. Tel.: +32-162-875-22; fax: +32-162-875-22.

E-mail address: loic.tous@imec.be

1. Introduction

Standard front side metallization of industrial silicon solar cells is based on printed silver paste contacts which are typically fired through a SiNx:H antireflection coating (ARC) for contact formation.

Contact resistance limitations for P surface concentrations $< 1 \times 10^{20}$ P atoms/cm³ and rather wide contact lines limit the range of compatible homogeneous emitters to surface concentrations (Ns) above 1×10^{20} P atoms/cm³ and to sheet resistance values below 90 Ω /sq [1]. This further limits cell efficiencies as high performance homogeneous emitters require low Ns [2]. An additional concern for silver based contacts is the relatively high cost of silver that is likely to increase as demand and supply issues increase driven by a fast expanding PV market. Similar reasoning is reflected in ITRPV [3] predictions which predict an average drop to 1/3 in Ag consumption per cell from 2010 to 2015 and further reductions beyond.

Using a two-layer approach [4] it is possible to overcome many of the limitations of printed Ag contacts. The first metal layer is chosen for its contact properties while the second metal layer is optimized for its current transport properties. Nickel is an excellent choice for the first layer for several reasons. First, it can be plated selectively in very narrow openings to form self-aligned contacts. Laser technologies allow the selective opening of lines in the ARC layer down to 10 μ m [5] enabling narrow contacts after Ni/Cu plating and hence reduced shadowing losses. Second, upon sintering nickel reacts with Si to form nickel silicides with very low specific contact resistance [6-7]. This enables the use of high efficiency emitters with low Ns. Finally, it has been shown to serve as an effective diffusion barrier for copper in PV modules [8]. Copper is an ideal candidate for the second layer because it is much cheaper and has a similar conductivity as silver enabling potentially lower processing costs [9].

Excellent cell results of self-aligned Ni/Cu contacts have been reported using simplified patterning schemes for the SiNx:H ARC layer. The most relevant ones are: laser ablation of the ARC [10-12], laser chemical processing [13-14], and laser doped selective emitters [15]. However, in most cases the pull tab adhesion of those contacts after standard tab soldering is not mentioned and/or is poor.

The purpose of this paper is to report on work using self-aligned Ni/Cu contacts including respective pull tab adhesion results on finished devices.

2. Experimental

In this work 1-3 Ω .cm, *p*-type, pseudo-square, 12.5 x 12.5 cm² Cz-Si (100) wafers with a starting thickness of 180 μ m were used. After random pyramid texturing and polishing of the rear side, the wafers were processed in two separate experiments according to the sequences described in Fig.1. Since both sequences feature different emitters, different laser ablation, and different plating sequences the purpose of this paper is to report on work using both sequences rather than comparing them one to another.

In a first experiment, solar cells comprising an industrial type 60 Ω /sq emitter ($N_s > 1 \times 10^{20}$ at/cm³) were processed into PERC type solar cells. Prior to POCl₃ diffusion, a SiO₂ diffusion mask was deposited at the rear side by means of chemical vapor deposition (CVD). The POCl₃ diffused emitter was passivated with a PECVD SiNx:H layer. At the rear side a PECVD SiNx:H layer was applied on top of the CVD SiO₂ diffusion mask. Local Al back-surface-field (BSF) contacts on the rear surface were formed using laser ablation of the backside dielectric layers, followed by physical vapor deposition (PVD) of Al, and a firing step in an inline belt furnace. This sequence results in so called i-PERC (industrially applicable Passivated Emitter and Rear Contact) solar cells [16-17]. Such solar cell structures are used in both experiments. In both cases the front contact is formed after forming the local rear contacts. For the 60 Ω /sq emitter the dielectric layer on the front (SiNx:H) was opened using a ns-UV laser ($\lambda=355$ nm) leading to contact openings of ~ 35 μ m. Finally, the solar cells were Ni/Cu/Ag plated in an industrial in-line tool from Meco and annealed in N₂ in a rapid thermal annealing (RTA) furnace. Ni (~ 1 μ m) was deposited by light

induced plating (LIP) (solution based on Ni sulfamate), Cu ($\sim 10\mu\text{m}$) and Ag capping ($\sim 1\mu\text{m}$) were electroplated. RTA was performed at 300°C .

In a second separate experiment, the process sequence was optimized and several changes were made. First, the standard $60\ \Omega/\text{sq}$ emitter was replaced by a high efficiency deep homogeneous $120\ \Omega/\text{sq}$ emitter ($N_s \sim 1 \times 10^{19}\ \text{at}/\text{cm}^3$) with thermal oxide passivation. To benefit from the thermal oxidation of both sides the SiO_2 diffusion mask was removed during the PSG etch. Subsequently, the rear $\text{SiO}_x/\text{SiN}_x$ dielectric stack was completed by means of PECVD. The laser ablation of the front $\text{SiO}_x/\text{SiN}_x:\text{H}$ dielectric stack has in that case been performed by a ps-laser leading to narrower contact openings of $\sim 12\ \mu\text{m}$. Contrary to the previous experiment, the RTA step to create self-aligned nickel silicide contacts was performed by sintering a thin PVD Ni layer prior to the final Ni/Cu/Ag plating sequence. One advantage of having the RTA step first is that potential Cu diffusion into the emitter during the sintering step is avoided. The final Ni/Cu/Ag plating sequence was performed at Imec using batch tools. Ni was deposited by LIP (solution based on Ni sulfamate), Cu was electroplated, and a solderable Ag cap was deposited by immersion.

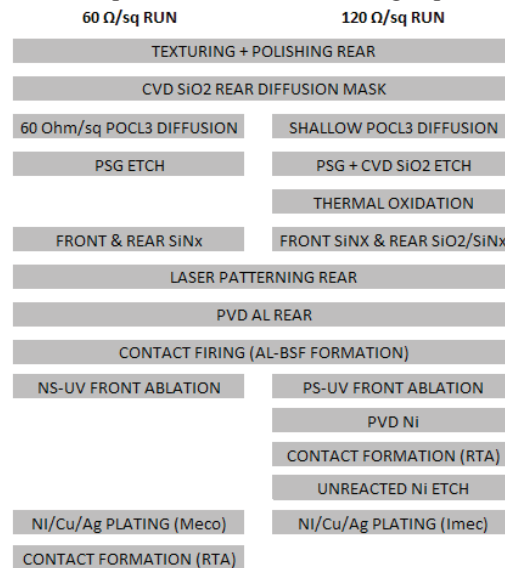


Figure 1: Process sequence for i-PERC solar cells featuring $60\ \Omega/\text{sq}$ and $120\ \Omega/\text{sq}$ emitters, respectively

3. Results and discussions

3.1. Electrical results with $60\ \Omega/\text{sq}$ emitters and ns-laser ablation

Table 1 gives average and best solar cell results achieved with the $60\ \Omega/\text{sq}$ i-PERC sequence.

Table 1. Average and best solar cells result on $160\ \mu\text{m}$ thick, $1\text{--}3\ \Omega\text{cm}$, pseudo-square $12.5 \times 12.5\ \text{cm}^2$, p -type CZ-Si wafers, $60\ \Omega/\text{sq}$ i-PERC solar cells with Ni/Cu/Ag contacts plated at Meco.* *Independently measured at FhG-ISE Cal-Lab*

Device	Jsc [mA/cm ²]	Voc [mV]	FF [%]	Eta [%]	Rseries [$\Omega\cdot\text{cm}^2$]	pFF [%]
average	38.3	649.1	75.8	18.9	1.1	81.9
(3 cells)	± 0.1	± 1.9	± 1.4	± 0.4	± 0.4	± 0
best*	38.5	648.5	75.6	18.9	0.90	81.9

As can be seen from Table 1, the electrical performance of the Ni/Cu/Ag contacts processed at Mecro is very encouraging with average V_{oc} close to 650 mV and average J_{sc} of 38.3 mA/cm². The good J_{sc} is the result of reduced shading losses thanks to the narrower plated contacts (~65 μ m). The high V_{oc} could be caused by incomplete laser ablation of the SiNx:H ARC. The reduced contact area would increase the contact resistance, and hence explain the poor FF values, and lead to lower recombination losses. Focused Ion Beam (FIB) cutting was used to create cross-sectional images of the plated lines by Scanning electron microscopy (SEM) as shown in Fig. 2.

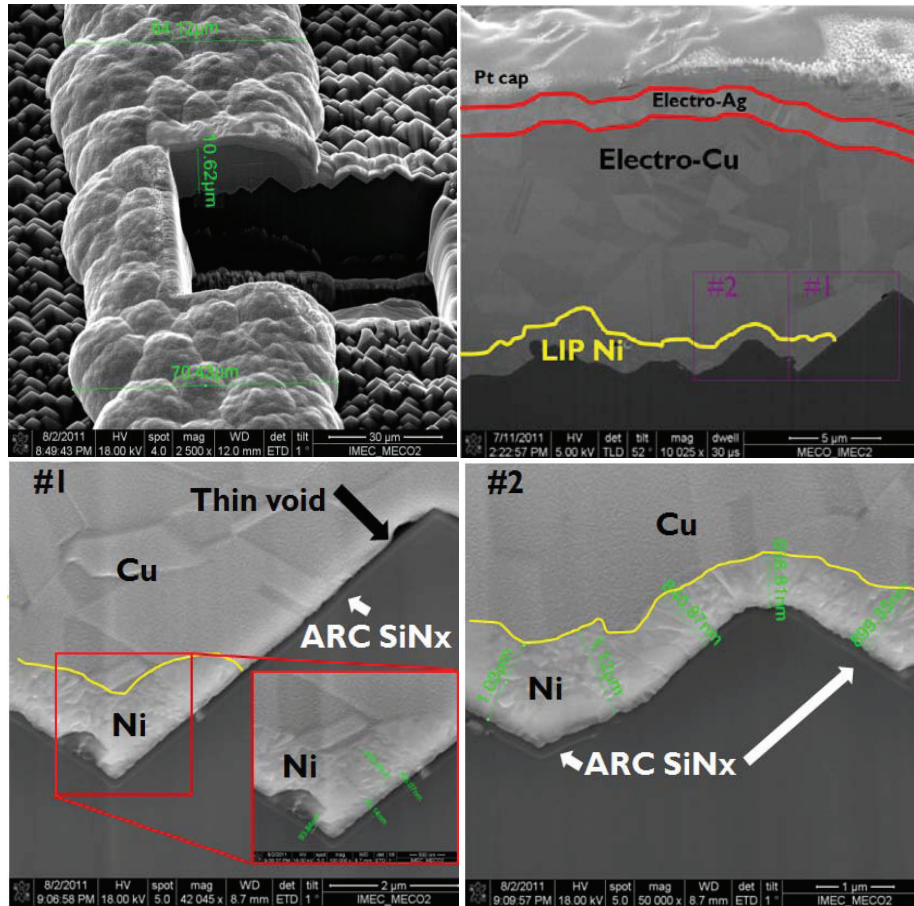


Fig. 2. (a) SEM image and FIB cut of a Ni/Cu/Ag contact plated at Mecro. (b) FIB cross section featuring the LIP Ni barrier, the electroplated Cu, and the electroplated Ag cap. (c) Zoom-in of square #1 present in Fig. 2(b). (d) Zoom-in of square #2 present in Fig. 2(b).

From these SEM images, the challenges of good line adhesion and creating a barrier to Cu diffusion become clear. Cu plating occurs in both lateral and vertical direction (contact opening is ~35 μ m, final Cu plated width is ~65 μ m). Cu does not adhere to SiNx as can be seen by the thin void present in Fig. 2(c) between the SiNx and Cu. As a result, less than half of the total line width can contribute to the line adhesion. Moreover, the selective ns-UV laser ablation of the SiNx:H layer is incomplete in many areas and especially at the edge of the laser opening (see Fig. 2(d)) leading to a reduced contact area. Non-

uniform ablation of SiNx on random pyramid textured surfaces has previously been reported with ns-laser ablation [10] and believed to be caused by optical effects within pyramids.

3.2 Electrical results with deep 120 Ω/sq emitters and ps-laser ablation

A batch of 4 cells with a deep 120 Ω/sq was processed according to the process flow described in Fig.1. Their average electrical performance as well as the best performing cell under standard illumination is given in table 2.

Table 2. Average and best illuminated I-V results of 12.5x12.5 cm² pseudo square Cz-Si 1.5 $\Omega\cdot\text{cm}$, PERC solar cells with 120 Ω/sq emitter and Ni/Cu/Ag contacts processed at Imec.

Device	Jsc [mA/cm ²]	Voc [mV]	FF [%]	Eta [%]	Rseries [$\Omega\cdot\text{cm}^2$]	pFF [%]
average (4 cells)	38.0 ± 0.2	646.5 ± 6.5	78.4 ± 0.4	19.3 ± 0.2	0.61 ± 0.02	81.8 ± 1.0
best	38.3	655.9	77.8	19.6	0.63	81.0

Table 2 shows that energy conversion efficiencies up to 19.6% were achieved with this process on large area (12.5x12.5 cm²) solar cells processed at Imec. The average FF was 78.4 \pm 0.4% and the average R_{series} was 0.61 \pm 0.02 $\Omega\cdot\text{cm}^2$ demonstrating the good reproducibility of the plating sequence. The average pFF was 81.8% indicating that further optimization of the laser ablation and the contact formation is required to deliver higher pFF values. Nevertheless, the fact that low R_{series} values were achieved with laser openings of \sim 12 μm demonstrates the excellent contact resistance properties of the nickel silicide contacts formed with PVD Ni. On the other hand, despite the very narrow lines formed (average \sim 40 μm after plating) no J_{sc} improvement was observed as compared to the 60 Ω/sq cell processed at Mecro. Two reasons for this lower J_{sc} have been identified so far. First, the measured shading loss for the best 120 Ω/sq cell was 6.9% as compared to 5.3% for the best 60 Ω/sq cell. This can be explained by the additional number of fingers that is required for the 120 Ω/sq cells to compensate for the emitter resistance loss between fingers. This translates in a 0.6 mA/cm² absolute loss in J_{sc} and should be reduced by further optimization of the plating thickness and contact pattern. Second, the 120 Ω/sq cell only gave a minor improvement in the short wavelength response as compared to the 60 Ω/sq cell as shown in the IQE measurements in Fig. 3. This indicates that even higher J_{sc} should be achievable with further optimization of the emitter formation, passivation and plating.

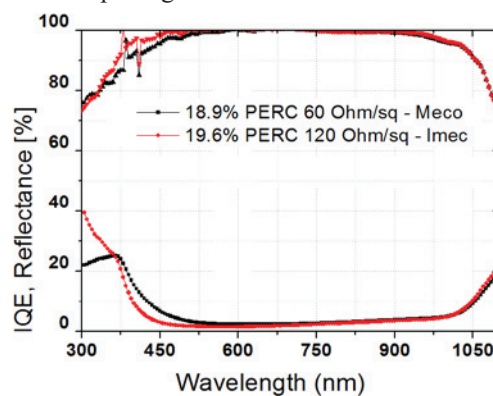


Fig. 3. IQE and reflectance comparison of 60 Ω/sq PERC cell processed at Mecro and 120 Ω/sq PERC cell processed at Imec.

3.3 Adhesion results with deep 120 Ω /sq emitters and ps-laser ablation

To study the adhesion of the Ni/Cu/Ag contacts plated at Imec we measured adhesion on the finished 120 Ω /sq solar cells described above. Standard Pb/Sn/Ag coated Cu ribbons (2x0.127 mm²) were hand soldered on the 1.2 mm wide busbars, and pulled off at a 45° angle. The force required to remove each solder joint was recorded. We obtained an average (over 29 points) of 2.0±0.7 N. This demonstrates that metal contacts having good adhesion can be achieved with the plating sequence developed at Imec.

Additionally, we measured soldered tab adhesion for a large set of full-Al BSF solar cells processed with the same Ni/Cu/Ag plating sequence. The soldering temperature was varied and two types of Pb/Sn/Ag coated Cu ribbons were used: a standard ribbon (2x0.127 mm²) and a thinner ribbon (2.0x0.100 mm²). Adhesion results are shown in Fig.4.

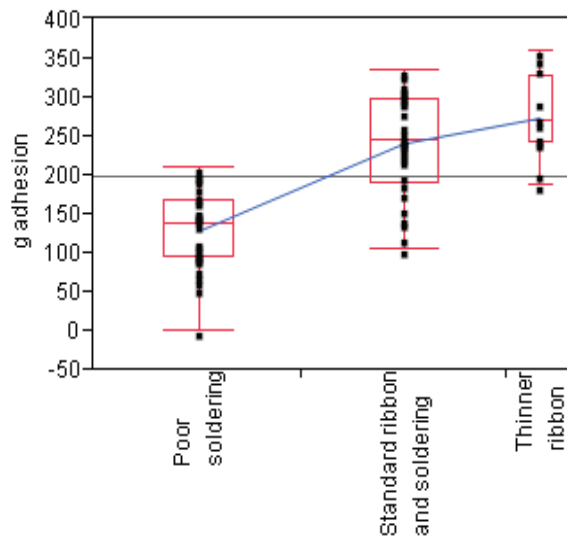


Fig. 4. Pull tab adhesion results under a 45° angle for Ni/Cu/Ag plated contacts under different soldering conditions

It is clear from these results that “poor” soldering conditions (too high soldering temperature) lead to lower adhesion results with average pull strength around 1.5 N as compared to the 2.5 N obtained with standard soldering temperatures. On the other hand, using a thinner ribbon, and hence imparting less stress to the cell on soldering, increased average pull strengths to approximately 2.7 N. This shows there is a strong impact of tabbing material as well as soldering conditions on adhesion results.

4. Conclusions

Current standard industrial solar cells with screen printed silver contacts limit the use of homogeneous emitters to those that are non-optimal due to the poor contact resistance at low Ns. Poor line conductivity and aspect ratio further limit efficiency. Coupled with the high price of silver, and potential future supply issues, strong motivations to look for alternatives arise.

Self-aligned Ni/Cu contacts appear a good alternative. In this work we reported on self-aligned Ni/Cu contacts formed by laser ablation of the ARC and subsequent Ni/Cu plating steps. Using ps-laser ablation we could form narrow openings of ~12 μ m leading to final contacts widths below 40 μ m after plating. Using this process we achieved energy conversion efficiencies up to η =19.6% on large area (12.5x12.5 cm²) CZ-Si *p*-type PERC cells using a 120 Ω /sq homogeneous emitter. Additionally, average pull tab

adhesion results >2 N were measured on those solar cells demonstrating that Ni/Cu contacts having good adhesion can be achieved with the plating sequence developed at Imec

Ultimately, copper metallization also needs to be shown to be cost effective together with persuasive short term reliability testing predicting long term stability.

Acknowledgements

The authors would like to thank C. Drijbooms for the FIB preparation and SEM images. The authors greatly acknowledge the support of the Imec Industrial Affiliated Partner (IIAP-PV) program. The support of S. Singh for PVD processing, of J. Beckers and J. Bertens for plating at Meco, is also greatly acknowledged.

References

- [1] Beaucarne G, Hoornstra J, Schubert G. Lessons from the Second Workshop on Metallization of Crystalline Silicon Solar Cells. *Future of Photovoltaics*, 2010, 1.
- [2] Sanchez MC, Stem N. Phosphorus Emitter and Metal - Grid Optimization for Homogeneous (n+p) and Double-Diffused (n++n+p) Emitter Silicon Solar Cells, *Materials Research*, 2009, Vol. 12, No. 1, p. 57-62.
- [3] www.itrpv.net.
- [4] Glunz SW, Mette A, Alemán M, Richter PL, Filipovic A, and Willeke GP. New concepts for the front side metallization of silicon solar cells, *Proc. of the 21st EUPVSEC*, Dresden, Germany, 2006.
- [5] Das J, Tous L, Hernández JL, Jaffrennou P, Ngamo M, John J, Posthuma NE, Baert K, and Poortmans J. Laser ablation: towards advanced industrial solar cell metallization processes, *Proc. of the 26th EUPVSEC*, Hamburg, Germany, 2011.
- [6] Braun S, Emre E, Raabe B, and Hahn G. Electroless nickel and copper metallization: contact formation on crystalline silicon and background plating behavior on PECVD SiNx:H layers, *Proc. of the 25th EUPVSEC*, Valencia, Spain, 2010.
- [7] Tous L, Recaman-Payo M, Ngamo M, Hernandez J-L, Poortmans J, and Mertens R. Evaluating contact resistance using epitaxially grown phosphorus emitters, *Proc. of the 26th EUPVSEC*, Hamburg, Germany, 2011.
- [8] Bruton T, Mason N, Roberts S, Nast Harley O, Gledhill S, Fernandez J, Russell R, Warta W, Glunz SW, Schultz O, Hermle, M, Willeke GP, Towards 20% efficient silicon solar cells manufactured at 60 MWp per annum, *Proc. of the 3rd WCPEC*, Osaka, Japan, 2003.
- [9] Kamp M, Bartsch J, Nold S, Retzlaff M, Hörteis M, Glunz SW. Economic Evaluation of Two-Step Metallization Processes for Silicon Solar Cells, *Proc. of the 1st Int. SiliconPV Conf.*, Freiburg, Germany, 2011.
- [10] Knorz A, Peters M, Grohe A, Harmel C, and Preu R. Selective laser ablation of SiNx layers on textured surfaces for low temperatures front side metallization, *Progress in Photovoltaics Res. Appl.*, 2009; 17, p. 127–136.
- [11] Alemán M, Bay N, Barucha D, Knorz A, Biro D, Preu R, and Glunz SW. Advances in electroless nickel plating for the metallization of silicon solar cells using different structuring techniques for the ARC, *Proc. of the 24th EUPVSEC*, Hamburg, Germany, 2009.
- [12] Tous L, van Dorp DH, Hernandez J-L, Allebe C, Ngamo M, Bender H, Meersschant J, Alemán M, Russell R, Poortmans J, and Mertens R. Minimizing junction damage associated with nickel silicide formation for the front side metallization of silicon solar cells, *Proc. of the 26th EUPVSEC*, Hamburg, Germany, 2011.
- [13] Kray D, Alemán M, Fell A, Hopman S, Mayer K, Mesec M, Müller R, Willeke GP, Glunz SW, Bitnar B, Neuhaus D-H, Lüdemann R, Schlenker T, Manz D, Bentzen A, Sauar E, Pauchard A, and Richerzhagen B. Laser-doped Silicon Solar Cells by Laser Chemical Processing (LCP) exceeding 20% Efficiency, *Proc. of the 33rd Photov. Spec. Conf.*, San Diego, USA, 2008
- [14] Kray D, Bay N, Cimiotti G, Kleinschmidt S, Kösterke N, Lösel A, Lühn O, Sailer M, Träger A, Kühnlein H, and Nussbaumer H. High efficiency large area industrial LCP selective emitters solar cells ready for production, *Proc. of the 25th EUPVSEC*, Valencia, Spain, 2010.
- [15] Hallam B, Wenham S, Sugianto A, Mai L, Chong C, Edwards M, Jordan D, Fath P. Record large area p-type CZ production cell efficiency of 19.3% based on LDSE technology, *Proc. of the 36th IEEE Photov. Spec. Conf.*, Seattle, USA, 2011.

- [16] Agostinelli G, Choulal P, Dekkers HFW, Ma Y, and Beaucarne G. Silicon solar cells on ultra-thin substrates for large scale production, *Proc. of the 21st EUPVSEC*, Dresden, Germany, 2006.
- [17] Prajapati V, Joachim J, Yang X, Mischke W, Hong J. Silane free high efficiency industrial silicon solar cells using dielectric passivation and local BSF, *Proc. of the 25th EUPVSEC*, Valencia, Spain, 2010.